

The Stability of Standing Waves with Small Group Velocity

Hermann Riecke

*Department of Engineering Sciences and Applied Mathematics
Northwestern University, Evanston, IL 60208, USA*

Lorenz Kramer

Physikalisches Institut, Universität Bayreuth, D-95440 Bayreuth, Germany

We determine the modulational stability of standing waves with small group velocity in quasi-one-dimensional systems slightly above the threshold of a supercritical Hopf bifurcation. The stability limits are given by two different long-wavelength destabilisation mechanisms and generically also a short-wavelength destabilisation. The Eckhaus parabola is shifted off-center and can be convex from below or above. For nonzero group velocity the Newell criterion, which near the cross-over from standing to traveling waves becomes a rather weak condition, does not determine the destabilisation of all standing waves in one dimension. The cross-over to the non-local equations that are asymptotically valid near threshold is discussed in detail. Close to the transition from standing to traveling waves complex dynamics can arise due to the competition of counter-propagating waves and the wavenumber selection by sources. Our results yield necessary conditions for the stability of traveling rectangles in quasi-twodimensional systems with axial anisotropy and form a starting point for understanding the spatio-temporal chaos of traveling oblique rolls observed in electroconvection of nematic liquid crystals.

I. INTRODUCTION

In this work the coupled complex Ginzburg-Landau equations

$$\partial_t A + u \partial_y A = \mu A + (1 + ib_2) \partial_y^2 A - c|A|^2 A - h|B|^2 A, \quad (1)$$

$$\partial_t B - u \partial_y B = \mu B + (1 + ib_2) \partial_y^2 B - c|B|^2 B - h|A|^2 B, \quad (2)$$

describing the interaction of two counterpropagating waves arising via a supercritical Hopf bifurcation in one space dimension (see e.g. [1]) are investigated. Here A and B are the complex wave amplitudes (or envelopes). The coefficients c and h are complex (we write $c = c_r + ic_i$ etc.) with $c_r > 0$ and $c_r + h_r > 0$ (see below), all other coefficients are real. The (dimensionless) control parameter μ (> 0 above threshold) carries the system across the instability. Time and length are scaled such that the diffusion constant is 1 [2]. Uniform scaling of Eqs.(1,2) with $\mu^{3/2}$ will be obtained by introducing slow variables $T = \mu t$ and $Y = \mu^{1/2} y$, and scaling A, B , and the group velocity u with $\mu^{1/2}$. Strictly speaking this requires u to be small of order $O(\mu^{1/2})$. While we focus on this case, we also discuss the case $u = O(1)$ as well as the cross-over between the two cases. We expect that our results will give insight into the case $u = O(1)$ somewhat further above threshold.

The spatially varying part of the physical fields \mathbf{u} are given in terms of these variables as

$$\mathbf{u} = \mu^{1/2} e^{i\hat{\omega}_h \hat{t}} \left(A(y, t) e^{i(\hat{p}_c \hat{y})} \mathbf{f}_1(x, z) + B(y, t) e^{i(-\hat{p}_c \hat{y})} \mathbf{f}_2(x, z) \right) + O(\mu) + c.c. \quad (3)$$

where $\hat{\omega}_h$ is the frequency of the fastest-growing linear mode, which at threshold ($\mu = 0$) is the Hopf frequency, \hat{p}_c the critical wavenumber and $\mathbf{f}_{1,2}(x, z)$ eigenfunctions of the linear problem. The hatted quantities (e.g. \hat{t}) are unscaled physical quantities.

In the case $h_r > c_r$ the two waves suppress each other and one often needs to consider only a single equation describing a traveling wave train. In many cases the group velocity term can then be discarded by going into a moving frame. The remaining equation has been studied intensely. In particular it is well known that the plane-wave solutions with wave number p_0 are stable with respect to long-wave side-band perturbations inside the band restricted by

$$1 + \frac{b_2 c_i}{c_r} - 2 \frac{(1 + (c_i/c_r)^2) p_0^2}{c_r F_{TW}^2} > 0, \quad (4)$$

where $F_{TW} = \sqrt{\mu - p_0^2}/c_r$ is the amplitude of the wave. Thus the band center solution $p_0 = 0$ is the last to lose stability when the Newell criterion $c_r + b_2 c_i > 0$ becomes violated [3,4]. In addition, for strong dispersion short-wave side-band perturbations can be important [4,5]. This occurs only for wavenumbers away from the band center and when the Newell criterion is satisfied ($c_r + b_2 c_i > 0$). It is not relevant in the following.

The coupled equations become important when h_r^2 becomes smaller than (or only slightly larger than) c_r^2 and then the superposition of oppositely traveling waves, leading to standing-wave solutions, becomes important. The stability of standing waves with respect to side-band perturbations has been studied so far only in a few special cases [6,7,8,9,5]. The case $u = 0$ and $h_i/h_r = c_i/c_r$ has been investigated in quite some detail in the context of polarized lasers [6]. There, however, the effects discussed below do not arise. For general values of the coefficients the solution in the center of the wave-number band has been investigated, for which the stability analysis is substantially simplified [7,8]. In addition to a long-wave instability an instability arising first at a finite perturbation wavenumber has been identified. The nonlinear evolution of the long-wave instability has been studied using coupled phase equations [7,8]. The evolution arising from the instability at finite wavenumber has been studied through numerical simulations of the Ginzburg-Landau equations [8]. The behavior away from the band center has not been studied in detail. From previous work we know, however, that the instability of the band-center solution may not always reflect the behavior of the solutions with other wave numbers [10]. We therefore present here a comprehensive analysis of standing waves for the complete band of wave numbers.

We know of no physical (quasi-) onedimensional system in which standing waves have been clearly observed. In thermal convection of binary mixtures in porous media in the Hopf bifurcation range rather strong oscillations of the Nusselt number have been observed [11], which can be taken as a hint for their occurrence in that system. Theoretically, a Hopf bifurcation to standing waves has been predicted for rotating convection at small Prandtl numbers [12].

In quasi-twodimensional systems with axial anisotropy an analogous situation arises when oblique rolls, i.e rolls appearing at an oblique angle with respect to the preferred axis, superpose to give traveling rectangles. In fact our investigation is motivated in particular by recent experiments on electroconvection in thin layers of nematic liquid crystals in the usual geometry with planarly aligned director, (see e.g. [13]) where in some parameter range Dennin et al. [14,15,16] found near onset extended small-amplitude spatio-temporal chaos characterized by the interaction of obliquely traveling waves (rolls) and defects in these waves. Figure 1 shows a typical state [14]. It consists of patches of waves traveling obliquely to the direction singled out by the anisotropy of the liquid crystal and their superposition, which can be considered as traveling rectangles [17]. A starting point for the understanding of this state of spatio-temporal chaos is therefore the consideration of the stability of traveling rectangles.

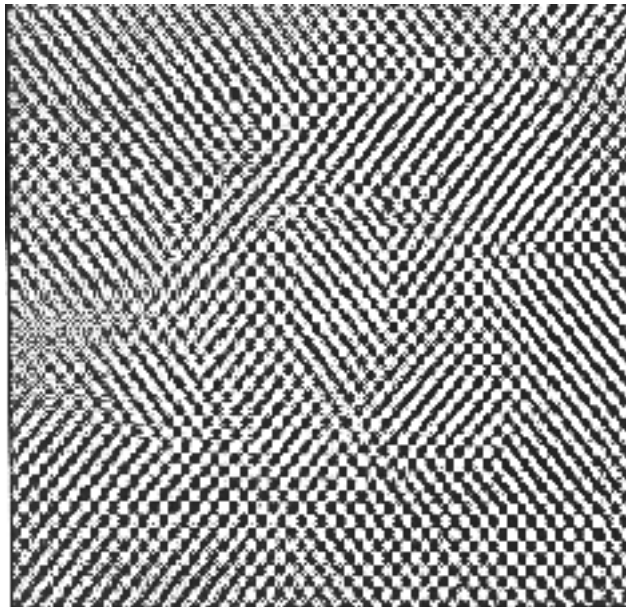


FIG. 1. Oblique waves ('zigs' and 'zags') and traveling rectangle patterns observed experimentally in electro-convection of nematic liquid crystals [14].

The liquid crystal system is axially anisotropic and the complex dynamics arises immediately above the onset of

convection in a supercritical bifurcation. Combined with the fact that the origin of the traveling waves in the liquid-crystal system is finally understood (on the basis of a weak-electrolyte model [18,19,20,21]) these features promise that the chaotic state may be understood *quantitatively* using equations which to a large extent can be dealt with analytically, i.e. Ginzburg-Landau equations.

A full, small-amplitude description of this system requires 4 complex modes for the left- and right-traveling waves in the 2 oblique directions. If one considers the common situation where oppositely traveling waves suppress each other strongly one is lead to two coupled Ginzburg-Landau equations,

$$\partial_t A + u \partial_y A = \mu A + (1 + ib_1) \partial_x^2 A + (1 + ib_2) \partial_y^2 A + 2a \partial_{xy}^2 A - c|A|^2 A - h|B|^2 A, \quad (5)$$

$$\partial_t B - u \partial_y B = \mu B + (1 + ib_1) \partial_x^2 B + (1 + ib_2) \partial_y^2 B - 2a \partial_{xy}^2 B - c|B|^2 B - h|A|^2 B. \quad (6)$$

In a restriction to modulations in the y -direction (1,2) are recovered. In this paper we therefore capture a subspace of the possible instabilities of traveling rectangles. For a quantitative comparison with the experiments the full twodimensional equations using parameters determined from the hydrodynamic equations [21] will be needed [22]. Presumably the onedimensional situation is also accessible experimentally by studying properly dimensioned narrow channels.

In Sec. II we study the stability of standing-wave solutions of Eq. (1,2). We find that, surprisingly, their stability is limited by two types of long-wave instabilities and a short-wave instability. One of the long-wave instabilities is related to the Eckhaus instability. Its parabolic stability limit is, however, shifted with respect to the neutral curve and can even be convex from above instead of below (see fig.2 below). The shift results from the linear group velocity term. Moreover, the stable solutions can be outside the Eckhaus parabola instead of inside. Not too far from the point of degeneracy between standing and traveling waves the Newell-type criterion for the instability of the band-center can be satisfied even for weak dispersion, but it does not indicate the loss of stability of standing waves at all wave numbers.

Thus the group velocity u plays an important role. In the general case of $u = O(1)$ the asymptotic validity of Eqs.(1,2) as $\mu \rightarrow 0$ has been questioned and in that limit equations have been proposed which are coupled through a term in which the counterpropagating wave is averaged over [23,24,25,26]. The long-wave stability properties of standing waves in these equations are found to differ markedly from those obtained from Eqs.(1,2). This has been demonstrated explicitly for the waves in the band center [24]. In Sec. III we show that the long-wave stability results of the non-local theory can be recovered from those of Eqs.(1,2) by taking the limit $\mu \rightarrow 0$ before allowing the wavenumber p of modulations to become small [24]. This corresponds to the situation in a finite system. The usual long-wave stability theory of Eqs.(1,2), on the other hand, amounts to $p \rightarrow 0$ in the infinite system. Strikingly, the cross-over from the result of the non-local equations to that of (1,2) can occur already very close to threshold.

II. THE STABILITY OF STANDING WAVES

The (unmodulated) standing-wave solutions of Eqs.(1,2) are given by

$$A = F e^{i(\omega t + p_0 y)}, \quad B = F e^{i(\omega t - p_0 y)} \quad (7)$$

with

$$F^2 = (\mu - p_0^2)/(c_r + h_r), \quad \omega = -u p_0 - b_2 p_0^2 - (c_i + h_i) F^2, \quad (8)$$

Clearly one needs $c_r + h_r > 0$ in order that the standing waves bifurcate supercritically. The neutral curve is given by $F^2 = 0$. Constant phases can be added to A and B separately.

The stability analysis with respect to side-band perturbations is based on the expansion

$$A = \left(1 + v_1 e^{\lambda t + i p y} + v_2 e^{\lambda^* t - i p y}\right) F e^{i(\omega t + p_0 y)}, \quad (9)$$

$$B = \left(1 + w_1 e^{\lambda t + i p y} + w_2 e^{\lambda^* t - i p y}\right) F e^{i(\omega t - p_0 y)}. \quad (10)$$

Inserting (9,10) into (1,2) yields after linearization in v_i and w_i a dispersion relation in the form of a quartic polynomial for $\lambda = \lambda(p)$ for given wave number p_0 and control parameter μ . Alternatively, through (8), the amplitude F can be considered as the control parameter. First of all, for $p = 0$, one finds a doubly degenerated eigenvalue $\lambda = 0$ corresponding to the two phase modes, and two amplitude modes with $\lambda = -2(c_r \pm h_r) F^2$. Thus the conditions

$c_r > 0$ and $c_r^2 > h_r^2$ are needed for amplitude stability. The long-wave expansion of the dispersion relation of the relevant phase mode

$$p = \epsilon p_1, \quad \lambda = \epsilon \lambda_1 + \epsilon^2 \lambda_2 + \dots, \quad \text{with } \epsilon \ll 1, \quad (11)$$

can be treated analytically. We find non-trivial instabilities at orders $O(\epsilon)$ as well as $O(\epsilon^2)$. Our analysis of those instabilities shows that quite generally one has to consider also instabilities at finite values of p . This is in contrast to the stability of traveling waves ($A = 0$ or $B = 0$) for which no instability occurs at order $O(\epsilon)$ and only in extreme cases a short-wavelength instability arises [4,5]. We have therefore also performed a general stability analysis by solving the quartic polynomial for λ numerically. It shows that despite the importance of short-wave instabilities the long-wave analysis provides over a wide range of parameters a framework for the overall structure of the stability regions.

In the long-wave expansion one finds at leading order in ϵ

$$\lambda_1^2 = -p_1^2 \frac{\alpha_1 \alpha_2}{c_r^2 - h_r^2} \quad (12)$$

with

$$\alpha_{1,2} = u(c_r \pm h_r) + 2p_0\{b_2(c_r \pm h_r) - (c_i \pm h_i)\}. \quad (13)$$

Thus, to this order the solution in the band center, $p_0 = 0$, is always stable since λ_1 is purely imaginary. In previous work [7,8] therefore no instability was found at this order. Such an instability arises, however, for $p_0 \neq 0$ (and $u \neq 0$) when the factors in the numerator of Eq.(12) change sign. As in a conservative system, the two imaginary eigenvalues then turn into two real eigenvalues, one positive and one negative, and lead to a steady instability. This occurs at

$$p_{0,1}^{(1)} = -\frac{u}{2} \frac{c_r - h_r}{b_2(c_r - h_r) + h_i - c_i}, \quad p_{0,2}^{(1)} = -\frac{u}{2} \frac{c_r + h_r}{b_2(c_r + h_r) - h_i - c_i}. \quad (14)$$

Note, that to this order the stability limit is independent of F and therefore also of μ . From (12) one finds that the standing waves are unstable outside the interval $(p_{0,1}^{(1)}, p_{0,2}^{(1)})$ and stable (to this order) inside that interval for $\gamma_1 < 0$ and vice versa, where

$$\gamma_1 \equiv (c_i - b_2 c_r)^2 - (h_i - b_2 h_r)^2 = u^2 \frac{c_r^2 - h_r^2}{4p_{0,1}^{(1)} p_{0,2}^{(1)}}. \quad (15)$$

Clearly this is equivalent to $p_{0,1}^{(1)}$ and $p_{0,2}^{(1)}$ having opposite or same sign, respectively. The stability limits (14) are sketched by dotted lines in fig.2.

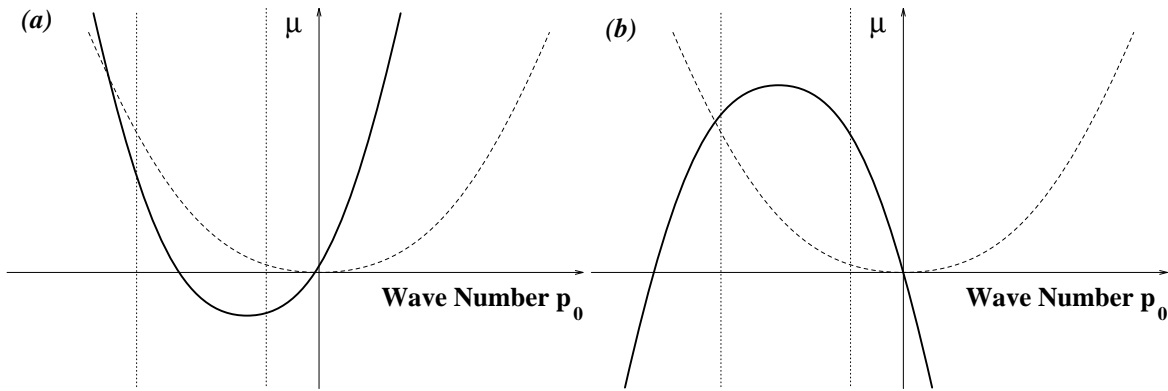


FIG. 2. Sketch of possible long-wave stability limits for standing waves. Standing waves are stable inside or outside the area delimited by the vertical dotted lines (instability at $O(\epsilon)$), depending on whether they exclude or include the band center, and inside or outside the parabolic area given by the heavy line ($O(\epsilon^2)$). The dashed line denotes the neutral curve.

At $O(\epsilon^2)$ one finds that either $\lambda_1 = 0$ or

$$\lambda_2 = p_1^2 \left\{ \beta_0 - \beta_1 \frac{p_0 u}{F^2} - \beta_2 \frac{p_0^2}{F^2} \right\} \quad (16)$$

with

$$\begin{aligned} \beta_0 &= \frac{b_2(h_r h_i - c_r c_i)}{c_r^2 - h_r^2} - 1, \\ \beta_1 &= \frac{2h_r(c_i h_r - c_r h_i)}{(c_r^2 - h_r^2)^2}, \\ \beta_2 &= 2 \frac{2b_2 h_r(c_i h_r - c_r h_i) - c_r(c_r^2 - h_r^2 + c_i^2 - h_i^2)}{(c_r^2 - h_r^2)^2}, \end{aligned} \quad (17)$$

and F^2 given by (8). The limit $p_0 \rightarrow 0$ ($\mu \neq 0$) agrees with previous results [7,8]. The Eckhaus-stability limit $\lambda_2 = 0$ is given by $\mu = \mu^{(eck)}(p_0)$ with

$$\mu^{(eck)} = \frac{\beta_1}{\beta_0}(c_r + h_r)up_0 + K^{(eck)}p_0^2 \quad \text{where} \quad K^{(eck)} = 1 + \frac{\beta_2}{\beta_0}(c_r + h_r). \quad (18)$$

In the parameter regime in which it is relevant ($\lambda_1^2 < 0$) the Eckhaus instability corresponds to an oscillatory instability and issues regarding its convective and absolute character arise.

The stability limits given by (16) have three remarkable properties.

i) At the band center $p_0 = 0$ the standing waves become unstable for $\beta_0 > 0$, i.e. for

$$b_2(h_r h_i - c_r c_i) + h_r^2 - c_r^2 > 0, \quad (19)$$

as already found in [7]. It was, however, not noted in that early work that this implies that near the transition from standing waves to traveling waves, $h_r \rightarrow c_r^-$, the solution at the band center becomes unstable for

$$b_2 c_i < b_2 h_i, \quad (20)$$

i.e. the condition involves only the imaginary parts b_2 , c_i , and h_i , and even very weak dispersion can be sufficient to destabilize the standing waves in this regime. This is to be contrasted with the result for traveling waves for which the solution in the band center becomes unstable only if the dispersion is sufficiently strong, as expressed by the Newell criterion $b_2 c_i < -1$ [3,4].

ii) The second striking feature is that the parabola giving the stability limit, $\mu = \mu^{(eck)}(p_0)$, is shifted with respect to the neutral curve as sketched in fig.2. This is due to the effect of the group velocity u . As a consequence, the instability of the solution at the band center does not imply the instability of all wave numbers (as one might have surmised in analogy with the case of traveling waves). Instead, when the solution with $p_0 = 0$ becomes unstable (cf. (19)), the apex of the parabola diverges to $\mu \rightarrow \pm\infty$ and the parabola merely flips over, becoming convex from above. Thus, an off-center band of wave numbers remains that is stable with respect to this instability (cf. fig.2b). Alternatively, when

$$K^{(eck)} = 0 \quad (21)$$

the parabola degenerates to a straight line and flips over in that way. In either case, for $u \neq 0$, there is always a range of wavenumbers (in particular for either small positive or small negative p_0) over which the solution is stable with respect to the Eckhaus instability even on the neutral curve. In certain parameter regimes those solutions with vanishing amplitude are also stable with respect to the conservative instability at $O(\epsilon)$ and therefore stable with respect to all long-wave perturbations. By continuity, however, the solution cannot be completely stable since the trivial state $F = 0$ is unstable. Therefore the long-wave analysis predicts that an instability has to arise which occurs first at a finite perturbation wave number. This is confirmed by the numerical evaluation of the dispersion relation $\lambda(p)$ (see below).

iii) In contrast to the case of traveling waves and that of steady patterns near threshold the stable standing-wave solutions do not have to lie inside the parabolic Eckhaus stability limit; the case in which the stable solutions are *outside* the Eckhaus parabola occurs as well. Since λ_2 can change sign only on the Eckhaus parabola and the neutral curve, the condition that the waves are unstable outside the parabola is given by $\beta_2 < 0$, i.e.

$$2b_2 h_r(c_i h_r - c_r h_i) - c_r(c_r^2 - h_r^2 + c_i^2 - h_i^2) < 0. \quad (22)$$

In the absence of dispersion this is always the case (since $c_r > h_r$). For sufficiently strong dispersion, however, λ_2 can become negative for large p_0 , and the waves are *stable outside* the parabola. Comparison with (15) shows that near the transition from standing waves to traveling waves, i.e. for $h_r \rightarrow c_r^-$, the behavior of the two instabilities is complementary at large $|p_0|$: either the pattern is unstable due to λ_1 or due to λ_2 . However, away from this transition *both* instabilities can arise for large p_0 or *neither*. The latter case is particularly interesting since it implies that the pattern is stable with respect to long-wave perturbations even on the neutral curve. This parameter regime is limited by the conditions $\gamma_1 = 0$ and $\beta_2 = 0$. Solving for b_2 and h_i one obtains

$$b_2^{(crit)} = -\frac{c_r}{2h_r} \frac{h_i^2 - c_i^2 + h_r^2 - c_r^2}{h_r c_i - c_r h_i} \quad (23)$$

and

$$h_i^{(1,2)} = (1/c_r) (c_i h_r \pm (c_r - h_r)|c|) \quad \text{or} \quad h_i^{(3,4)} = (1/c_r) (c_i h_r \pm (c_r + h_r)|c|). \quad (24)$$

This leads to three intervals in h_i over which $\lambda_1^2 < 0$ and $\beta_2 = 0$. For $h_r > 0$ they are given by $(-\infty, h_i^{(4)})$, $(h_i^{(2)}, h_i^{(1)})$ and $(h_i^{(3)}, \infty)$. For $h_r < 0$ the values $h_i^{(1,2)}$ and $h_i^{(3,4)}$ interchange their roles. In these intervals and for b_2 close to $b_2^{(crit)}$ the long-wave stability analysis suggests that the pattern is stable even on the neutral curve. Again, this indicates the appearance of an instability at finite wavelength (see below).

Thus, a number of qualitatively different situations can arise. For

$$K^{(eck)} > 0 \quad (25)$$

the parabola is convex from below and otherwise convex from above. In either case the solution in the band center is stable for

$$\beta_0 < 0. \quad (26)$$

If the parabola is convex from below this implies that the solution is stable inside the parabola, otherwise it is stable outside the parabola. In the former case it is worthwhile to consider the width of the Eckhaus-parabola. For

$$\beta_0 \beta_2 > 0 \quad (27)$$

it is narrower than the neutral curve and wider otherwise. This implies that β_2 determines the Eckhaus-stability of the solution with large $|p_0|$ (cf. (22)). In each of the cases the conservative instability at $O(\epsilon)$ can arise inside or outside the interval $(p_{0,1}^{(1)}, p_{0,2}^{(1)})$ as determined by γ_1 .

In figs.3-5 representative cases for the stability limits are shown as obtained from the long-wave results (12) and (16), and by numerically solving the dispersion relation $\lambda(p)$. In fig.3a the parabola is convex from below and the Eckhaus-stable solutions are inside. For the parameters chosen, the conservative instability destabilizes the solutions in a vertical strip inside that parabola. When the parameters are changed so as to render the band center unstable the parabola becomes convex from above and one obtains the situation given in fig.3b (Note the enlarged wavenumber scale). Only the small area between the parabola and the vertical stability limit corresponds to stable solutions. Since the long-wave instabilities do not arise on the neutral curve for small negative p_0 an instability at finite wavelength arises there. It is indicated by solid squares.

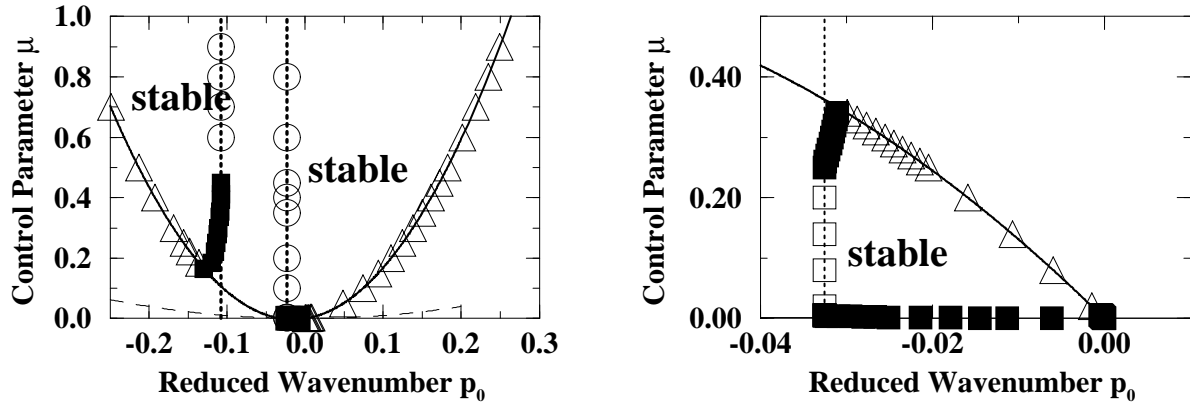


FIG. 3. Stability limits for standing waves. Long-wave expansion at $O(\epsilon)$ (dotted line) and $O(\epsilon^2)$ (solid line). The dashed line denotes the neutral curve. The symbols denote the stability limits as obtained from the numerical analysis of the dispersion relation $\lambda(p)$ with the solid squares marking an instability at finite perturbation wave number. The parameters are as follows: a) $c = 1 - 0.4i$, $h = 0.6 + 0.3i$, $b_2 = 0.4$, $u = 0.1$, b) $c = 1 - 0.6i$, $h = 0.7 + 0.6i$, $b_2 = 0.6$, $u = 0.3$.

In fig.4a the Eckhaus parabola is wider than the neutral curve. Since the $O(\epsilon)$ -instability destabilizes the solution only in the small range close to the band center the wavenumber band is limited by the finite-wavelength instability for large $|p_0|$. In fig.4b the stable solutions are outside the Eckhaus parabola and again perturbations at finite wavelength are important.

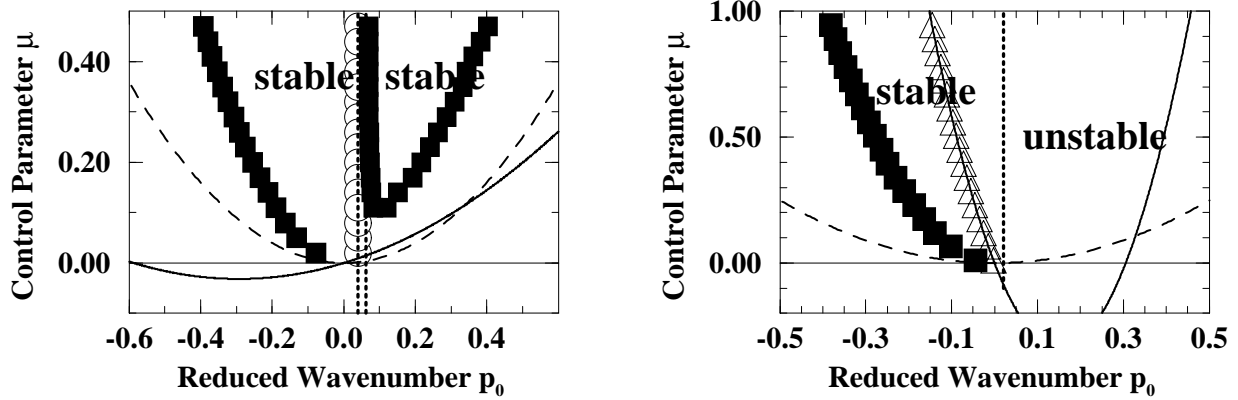


FIG. 4. Stability limits for standing waves (cf. fig.3). The parameters are as follows: a) $c = 1 + 0.3i$, $h = 0.5 + 0.5i$, $b_2 = -1.96$, $u = 0.2$, b) $c = 1 + 0.3i$, $h = 0.2 + 0.5i$, $b_2 = -4.85$, $u = 0.2$,

For the parameters chosen in fig.5a the stable solutions are also outside the parabola, but the parabola is now convex from above. In the final case, shown in fig.5b, the standing waves are again Eckhaus-stable outside the parabola, which is convex from below (cf. inset). Now the conservative instability limits the wavenumber band on the other side (compare with fig.4b) and only a very small region of stability remains.

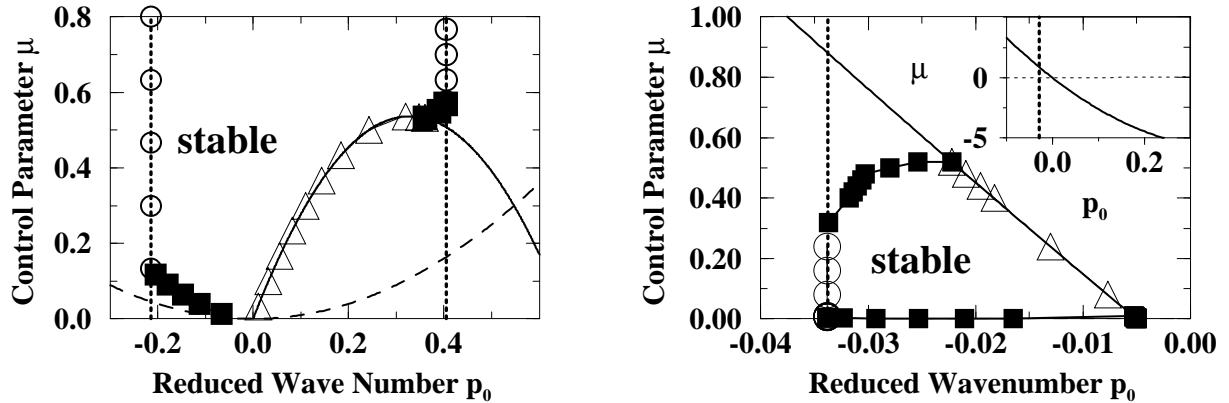


FIG. 5. Stability limits for standing waves (cf. fig.3). The parameters are as follows: a) $c = 1 - 0.3i$, $h = 0.7 + 0.7i$, $b_2 = -1$, $u = 1$, b) $c = 1 + 0.7i$, $h = 0.9 + 1.5i$, $b_2 = 0.7$, $u = 0.5$.

As indicated above, due to the finite group velocity there is generically a range of wave numbers for which the solution is stable on the neutral curve with respect to long-wave perturbations. Figs.3-5 confirm that therefore generically instabilities occur at finite perturbation wave number p . This is to be contrasted with the case of traveling waves where they appear only for sufficiently strong dispersion [4,5].

Let us briefly discuss the case of vanishing group velocity separately. As is apparent from (12) and (14) the stability

with respect to long-wave perturbations does not depend on the wavenumber p_0 to $O(\epsilon)$: either all wavenumbers are unstable ($\gamma_1 < 0$) or stable ($\gamma_1 > 0$). In the latter case the long-wave stability limits are determined by (18). At $O(\epsilon^2)$ one obtains a symmetric Eckhaus parabola. Again it can be convex down or up and can be wider or narrower than the neutral curve. Two cases are shown in fig.6a,b. In fig.6a the Eckhaus parabola is narrower than the neutral curve and the stability limit is indeed given by the long-wave instability. In fig.6b the parabola is wider and the stability is limited by a instability with finite p .

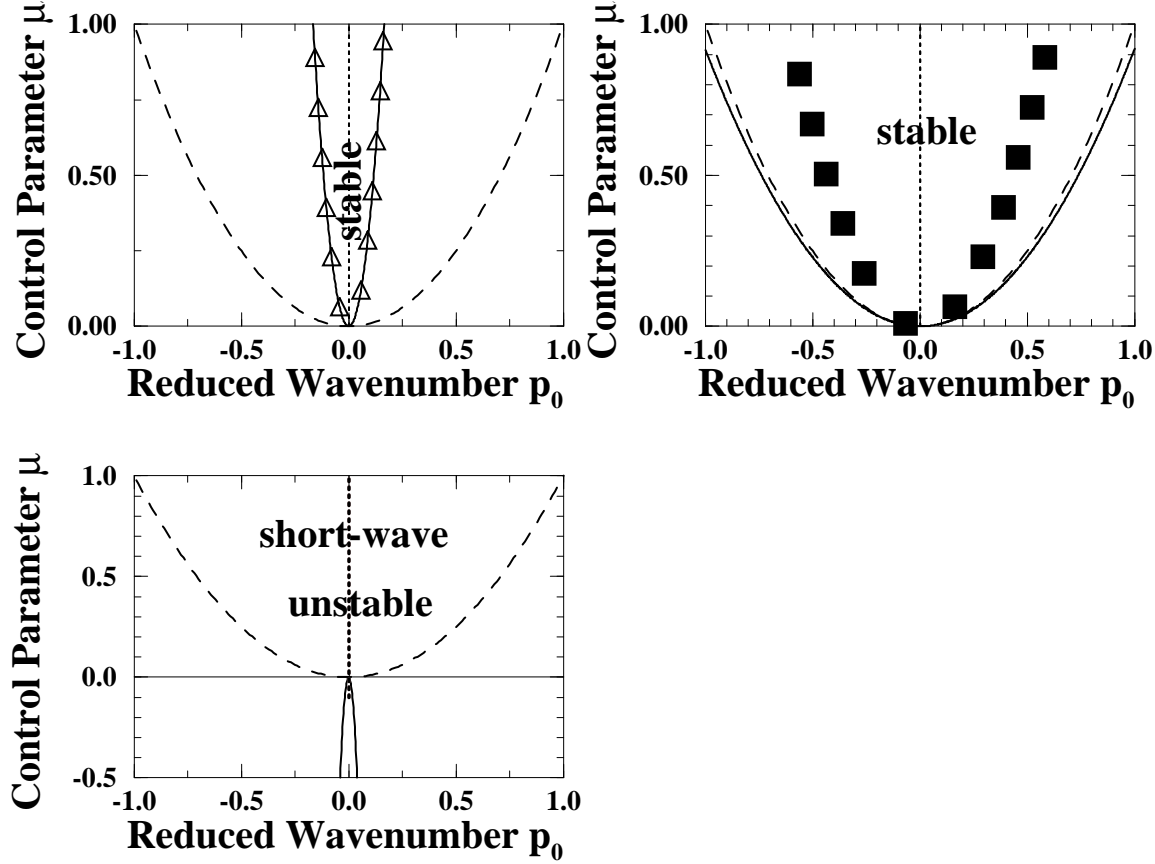


FIG. 6. Stability limits for standing waves with vanishing group velocity. Long-wave expansion at $O(\epsilon)$ (dotted line) and $O(\epsilon^2)$ (solid line), and instability at finite perturbation wave number (solid squares). The symbols denote the stability limits as obtained from the numerical analysis of the dispersion relation $\lambda(p)$. Neutral curve given by dashed line. Note that in c) *all* wavenumbers are *stable* according to the long-wave analysis, but they are in fact all *unstable* due to an instability at finite p . The parameters are as follows: a) $c = 1 + 1.1i$, $h = 0.6 + 0.5i$, $b_2 = -0.5$, $u = 0$, b) $c = 1 + 1.1i$, $h = 0.6 + 0.5i$, $b_2 = 9$, $u = 0$,

For $u = 0$ the instability at finite p can be captured analytically near the band center because it arises there for $p = O(p_0)$. To that end the perturbation wavenumber p and the wavenumber p_0 are taken to be of the same order, i.e.

$$p = \epsilon p_1, \quad p_0 = \epsilon p_{01}, \quad \lambda = \epsilon \lambda_1 + \epsilon^2 \lambda_2 + \dots \quad (28)$$

At $O(\epsilon^2)$ one obtains $\lambda_1 = 0$. Note that (16) does therefore not apply and one has to go to higher order. At $O(\epsilon^4)$ one finds

$$\lambda_2^{(1,2)} = p_1^2 \beta_0 \pm p_1 \sqrt{W_1} \quad (29)$$

with

$$W_1 = \frac{b_2^2 (c_r h_i - c_i h_r)^2}{(c_r^2 - h_r^2)^2} p_1^2 - 4 \left(b_2^2 - 2 \frac{b_2 (c_r c_i - h_r h_i)}{c_r^2 - h_r^2} + \frac{c_i^2 - h_i^2}{c_r^2 - h_r^2} \right) p_{01}^2. \quad (30)$$

The limit $p_0 \rightarrow 0$ of the previous result (12),(16) for $\lambda_{1,2}$ is regained by taking the limit $p_1 \rightarrow 0$ in (29,30). Thus, if the first term in (29) is negative and the prefactor of p_{01}^2 in (30) is positive $\sqrt{W_1}$ is imaginary in the long-wave limit and the waves with small p_0 are stable. However, the first term in W_1 becomes important when the modulation wavenumber becomes larger. Thus, for $|p_1| \gg |p_{01}| > 0$ (29) yields an instability at a finite modulation wavenumber if $\beta_0 + \sqrt{W_1(p_{01}=0)} > 0$, i.e.

$$b_2(c_i - h_i) + c_r - h_r < 0, \quad \text{or} \quad b_2(c_i + h_i) + c_r + h_r < 0. \quad (31)$$

Such a case is shown in fig.6c in which all wavenumbers are stable with respect to long-wave perturbations ($\beta_0 < 0$, $\beta_2 > 0$, and $\gamma_1 > 0$), but all wavenumbers are *unstable* to perturbations at finite p_1 . Note, that the relevant perturbation wavenumber goes to 0 in the band center. In the special case $p_0 = 0$ the stability conditions (31) are therefore also obtained in a long-wave analysis [8].

III. ANALYSIS FOR LARGE GROUP VELOCITY

Recently there has been some discussion of the fact that equations (1,2) are not obtained in that form when a direct expansion of the microscopic equations like the Navier-Stokes equations is performed near threshold [9,23,24,25,26,27,28]. Since the group velocity of the waves is generically of $O(1)$ one is, strictly speaking, either led to consider a hyperbolic system without the second space derivatives in (1,2) [27,28] or to introduce two different time scales $T_1 = \epsilon t$ and $T_2 = \epsilon^2 t$ [9,23,24,25,26]. One then obtains already at quadratic order a solvability condition,

$$\partial_{T_1} A + u \partial_Y A = 0, \quad (32)$$

$$\partial_{T_1} B - u \partial_Y B = 0. \quad (33)$$

Solving these equations in the frames co-moving with the respective waves ($Y_{\pm} = Y \mp u T_1$) one then obtains at third order

$$\partial_{T_2} A = \mu A + (1 + i b_2) \partial_{Y_+}^2 A - c |A|^2 A - h < |B|^2 > A, \quad (34)$$

$$\partial_{T_2} B = \mu B + (1 + i b_2) \partial_{Y_-}^2 B - c |B|^2 B - h < |A|^2 > B, \quad (35)$$

with $< \dots >$ denoting spatial averages. These equations differ from (1,2) in particular in their non-local cross-coupling terms between A and B : At the band center the linear stability with respect to long-wave perturbations of the standing waves has been investigated within these equations and a result quite different from that obtained in sec.II has been obtained [24]. It has been pointed out that the difference between the two long-wave results is due to the fact that two limits have been taken: small amplitudes, i.e. $\mu \rightarrow 0$, and long waves, i.e. $p \rightarrow 0$. These two limits do not commute. It has been argued that the asymptotically correct sequence is to take first $\mu \rightarrow 0$, which leads to the non-local equations (34,35), and then $p \rightarrow 0$. It is therefore of great interest to understand the connection between the two results and in particular the respective regimes of relevance. As long as no long-wave limit is taken the local (reconstituted) equations are expected to be valid.

As discussed in [24] the stability result obtained from the non-local equations can be recovered from the local equations if the limit $\mu \rightarrow 0$ is considered before taking the long-wave limit. To extend the analysis presented in [24] away from the band center we consider the full 4th-order dispersion relation of perturbations of standing waves within the local equations taking the limit $\mu \rightarrow 0$ before considering the long-wave limit. Due to the parabolic character of the neutral curve the wave numbers have to be rescaled along with μ ,

$$\mu = \eta^2 \mu_2, \quad p_0 = \eta p_{01}, \quad p = \eta p_1, \quad F = \eta F_1. \quad (36)$$

The growth rates are also rescaled,

$$\lambda = i u p + \eta^2 \Lambda. \quad (37)$$

One then obtains at $O(\eta^6)$

$$\begin{aligned} \Lambda^2 + \Lambda (2p_1^2 - 4ip_{01}b_2p_1 + 2c_rF_1^2) - (1 + b_2^2)(4p_{01}^2 - p_1^2)p_1^2 \\ - 4i(c_r b_2 - c_i)p_1 p_{01} F_1^2 + 2(c_r + c_i b_2)p_1^2 F_1^2 = 0 \end{aligned} \quad (38)$$

Note that u , which is assumed to be $O(1)$, does not affect the (convective) destabilisation. Actually this dispersion relation coincides with that obtained for traveling waves, if F_1 is replaced by the traveling-wave amplitude. If one now expands in small perturbation wavenumbers p_1 , one obtains for the growth rate

$$\Lambda = 2ip_0p_1 \frac{-c_i + c_r b_2}{c_r} + p_1^2 \left(2 \frac{|c|^2}{c_r^3 F_1^2} p_{01}^2 - \frac{c_r + c_i b_2}{c_r} \right) + O(p_1^3). \quad (39)$$

Thus, in this limit no conservative instability arises and the stability boundaries are given by a parabolic curve. Note that the term in brackets corresponds to the negative of the expression in Eq.(4). In fact, the destabilization of all periodic solutions is indicated by the loss of stability of the solution in the band center which occurs for the same parameter values (as for the traveling wave),

$$b_2 c_i < -c_r. \quad (40)$$

This is in strong contrast to the result found in (16) above, where for non-vanishing group velocity the Eckhaus curve was shifted with respect to the neutral curve. None of the complex behavior discussed above is obtained in (34,35).

Central to the difference between the two stability results is the long-wave limit. To understand the connection between them it is useful to consider a distinguished limit in which μ and the perturbation wave number p are both small of the same order,

$$\mu = \epsilon^2 \mu_2, \quad p_0 = \epsilon^2 p_{02}, \quad p = \epsilon^2 p_2, \quad F = \epsilon F_1, \quad \lambda = iup + \epsilon^4 \lambda_4, \quad (41)$$

which differs from the previous limit (36) in the scaling of the modulation wavenumber p and that of the growth rate λ . It turns out that the wavenumber p_0 of the standing waves themselves has to be taken to be of $O(\epsilon^2)$ in order to obtain a single expression that reduces to the results of the local and of the non-local equations in suitable limits. At leading order ($O(\epsilon^9)$) one obtains then

$$\lambda_4 = \mathcal{N}^{-1} p_2^2 \left\{ 2F_1^2 h_r (c_r h_i - c_i h_r) u p_{02} - (c_r^2 - h_r^2) (c_r^2 - h_r^2 + b_2(c_r c_i - h_r h_i)) F_1^4 - u^2 c_r (c_r + b_2 c_i) p_2^2 \right\} + \\ + i \mathcal{N}^{-1} p_2 \left\{ 2(c_r^2 - h_r^2) (b_2(c_r^2 - h_r^2) + h_r h_i - c_r c_i) F_1^4 p_{02} + u p_2^2 (2u p_{02} c_r (c_r b_2 - c_i) - b_2 h_r (c_r h_i - c_i h_r) F_1^2) \right\} \quad (42)$$

$$\mathcal{N} = (c_r^2 - h_r^2) F_1^4 + u^2 p_2^2 c_r^2. \quad (43)$$

For small amplitudes F_1 (42) reduces to

$$\lambda_4 = -p_2^2 \frac{c_r + b_2 c_i}{c_r} + 2p_{02} h_r \frac{c_r h_i - c_i h_r}{u c_r^2} F_1^2 + i p_2 \left\{ 2p_{02} \frac{c_r b_2 - c_i}{c_r} - \frac{h_r b_2 (c_r h_i - c_i h_r)}{u c_r^2} F_1^2 \right\} + O(F_1^4). \quad (44)$$

This limit agrees to leading order with the result from the non-local theory (39). Note that due to the choice $p_0 = O(\epsilon^2)$ the wavenumber dependence of λ in the non-local theory (cf. (39)) does not appear to this order. In the limit of large amplitudes one obtains from (42)

$$\lambda_4 = p_2^2 \left\{ \beta_0 - \beta_1 \frac{p_{02} u}{F_1^2} \right\} + \\ + i p_2 \left\{ 2p_{02} \frac{b_2(c_r^2 - h_r^2) + h_i h_r - c_i c_r}{c_r^2 - h_r^2} + u p_2^2 \frac{h_r b_2 (c_r h_i - c_i h_r)}{(c_r^2 - h_r^2)^2 F_1^2} \right\} + O(F_1^{-4}) \quad (45)$$

with β_0 and β_1 defined in (17). Comparison with (12) and (16) shows that the limit (41) also reproduces to leading order the result from the local theory. The imaginary part corresponds to an expansion of λ_1 from (12) for small p_0 , noting that a term iup_2 has been split off in (41).

Thus, the distinguished limit (41) provides a connection between the two regimes and allows to give an expression for the parameters at which the cross-over occurs. Focussing on the band center, $p_0 = 0$, the stability is determined by the second and third term in (42). A reasonable definition for the cross-over is therefore their ratio Γ ,

$$\Gamma = \left| \frac{(c_r^2 - h_r^2)(c_r^2 - h_r^2 + b_2(c_r c_i - h_r h_i))}{c_r (c_r + b_2 c_i)} \right| \frac{F^4}{u^2 p^2}. \quad (46)$$

The non-local theory is appropriate for $\Gamma \ll 1$. For fixed values of the group velocity u , this corresponds to small amplitudes $F^2 \sim \mu$. The cross-over to the regime in which the results of the local theory are recovered occurs near μ_c , which is defined *via* $\Gamma = 1$. Eq.(46) shows that μ_c depends not only on the group velocity u but also on the wavenumber p of the relevant perturbations and therefore on the size $L = 2\pi/p_{min}$ of the physical system under consideration,

$$\mu_c \propto u p_{min}. \quad (47)$$

This dependence is illustrated in fig.7a. There the analytical results (18,39) are shown as well as the numerical result from the full dispersion relation for three system sizes corresponding to $p_{min} = 0.02$, $p_{min} = 0.01$, and $p_{min} = 0.005$. The other parameters are $c = 1 + 0.5i$, $h = 0.5 + 0.5i$, $u = 10$, and $b_2 = 0$. As expected, the non-local theory is correct for small μ . For larger μ strong deviations arise for $p_0 > 0$. They signify the cross-over to the result of the local equations. In agreement with (47), in longer systems the cross-over occurs at smaller values of μ . This illustrates the fact that the difference between the two approaches is due to the fact that the limits $\mu \rightarrow 0$ and $p \rightarrow 0$ are not interchangeable. In the limit $p \rightarrow 0$ at fixed μ one obtains the result of the local equations, whereas for $\mu \rightarrow 0$ at fixed p the result of the non-local equations are obtained. It is noteworthy, that the cross-over occurs at quite small values of μ even though the group velocity is quite large ($u = 10$). At the same time the instability for $p_0 < 0$ is not captured at all within the long-wave limit of the local equations. As discussed in sec.II, within the long-wave limit the waves would be stable all the way to the neutral curve, implying that a short-wave instability arises. Interestingly, although this instability appears in the local equations as a short-wave instability, it is captured correctly in the long-wave analysis of the non-local equations.

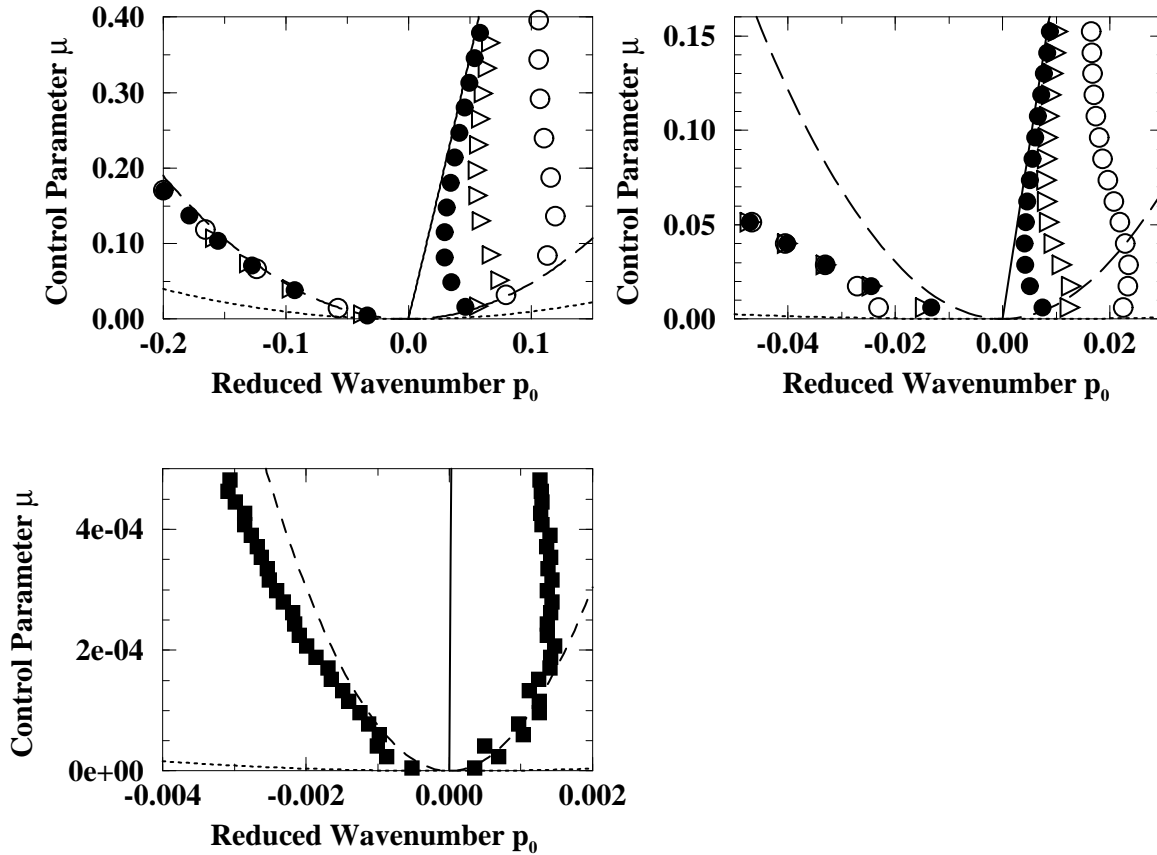


FIG. 7. Comparison between stability results from non-local (34,35) and local equations (1,2). Solid line from (18), dashed line from (39), dotted line gives the neutral curve. Symbols denote the stability limits from the full dispersion relation for $p_{min} = 0.02$ (open circles), $p_{min} = 0.01$ (triangles), $p_{min} = 0.005$ (solid circles), and $p_{min} = 0.0005$ (in c)). The parameters are $c = 1 + 0.5i$, $h = 0.5 + 0.5i$, $u = 10$, and $b_2 = 0$ (in a)) and $b_2 = -1.9$ (in b) and c)).

Eq.(46) suggests that the cross-over to the result of the local equations occurs at a lower value of μ if $c_r + c_i b_2$ is small, i.e. close to the Newell criterion (40) for the standing waves (within the non-local equations). This is demonstrated in fig.7b. There the stability limits are shown for the same parameters as in fig.7a except for b_2 which is here -1.9 . Thus, $c_r + c_i b_2 = 0.05$. As in the case $b_2 = 0$, the long-wave results of the local theory are adequate for long systems and larger μ (note the different scales as compared to fig.7a) for $p_0 > 0$. The long-wave stability limits obtained from the non-local equations deviate, however, quite strongly even at very small values of μ . Strikingly, before the parabolic dependence of the non-local result takes over when μ is decreased, additional deviations arise, which are due to the terms of $O(p^4)$ in (39). They are important for $\mu \leq \mu_f \propto p^2$. Of course, if the system size is

increased these deviations become smaller, but at the same time the cross-over is shifted to lower values μ_c , as well. More precisely, one has the scaling

$$\mu_f \propto p^2 \ll \mu_c \propto p \quad \text{for } p \ll 1. \quad (48)$$

Thus, for sufficiently large systems there always remains an intermediate regime in which the parabolic behavior from the non-local equations is relevant. It can, however, occur for values of μ that are extremely small. This is demonstrated in fig.7c which shows a blow-up¹ of fig.7b for $p_{min} = 0.0005$. The usual local Ginzburg-Landau equations contain this result and capture in addition the rich possibilities that can arise for larger values of μ .

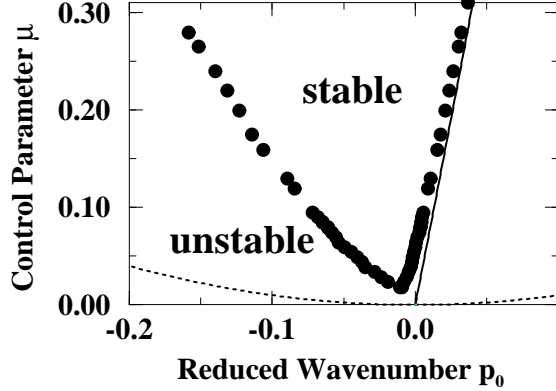


FIG. 8. Comparison between stability results from non-local (34,35) and local equations (1,2). Within the non-local equations all standing waves are unstable. Solid line from (18), dotted line gives the neutral curve. Symbols denote the stability limits from the full dispersion relation for $p_{min} = 0.005$ (solid circles). The parameters are $c = 1 + 0.5i$, $h = 0.5 + 0.5i$, $u = 3$, and $b_2 = -2.2$ (cf. fig.7).

A further interesting case is obtained if the Benjamin-Feir criterion $c_r + b_2 c_i$ is satisfied within the non-local equations. In that case all standing waves are unstable immediately at onset. At slightly larger values of the control parameter, however, the waves can become stable. This is shown in fig.8. Although with increasing values of the group velocity the gap of instability increases, it is seen that the restabilization can occur already for quite small values of the control parameter even for moderately large group velocity.

Of course, at larger values of μ higher-order corrections will have to be included. Since the expansion leading to (1,2) is only asymptotic (rather than convergent) firm predictions for *finite* values of μ cannot be made. However, if the cross-over to the local equations occurs for small values of μ it is quite reasonable to expect that the rich behavior displayed in figs.3-5 will not be strongly affected by the higher-order corrections.

IV. NUMERICAL SIMULATIONS IN THE UNSTABLE REGIMES

In order to determine the dynamics ensuing from the instabilities found analytically we have solved (1,2) numerically for a range of parameters. We have focussed in particular on the behavior in the vicinity of the transition from standing waves to traveling waves ($h_r \rightarrow c_r^-$), since in this regime even weak dispersion can lead to a destabilization of standing waves at all wavenumbers (cf. fig.3b). Figures 9-11 show a sequence of space-time diagrams for increasing values of h_r straddling the transition point $h_r = c_r$. As initial condition a slightly perturbed standing wave was chosen. The shades of gray in the space-time diagrams indicate the normalized difference $(|A| - |B|)/(|A| + |B|)$ between the amplitudes of the right- and left-traveling wave with bright areas indicating domains in which the right-traveling wave dominates and dark ones those in which the left-traveling wave dominates. For $h_r = 0.7$ both wave components are about equally strong resulting in a solution which corresponds mostly to a standing wave. This standing wave exhibits,

¹For these parameter values round-off errors produced some scatter in the data.

however, complex dynamics due to the persistent occurrence of phase slips in one of the two wave components and due to fairly localized disturbances propagating through the system.

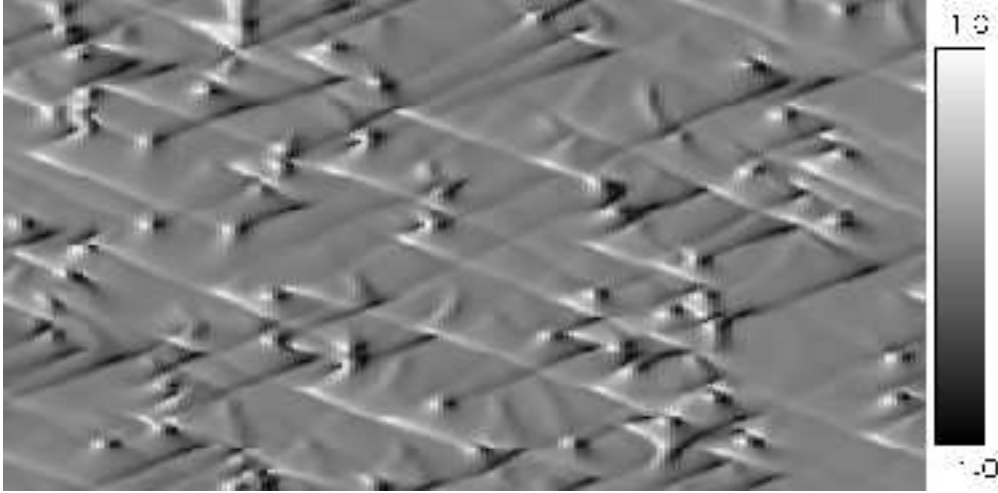


FIG. 9. Space-time diagram (space horizontally, time vertically upward) of evolution obtained by numerical simulation of (1,2) for $\mu = 0.4$, $c = 1 - 0.6i$, $h = 0.7 + 0.6i$, $b_2 = 0.6$, $u = 0.3$ (cf. fig.3b). The shades of gray indicate the normalized difference $(|A| - |B|)/(|A| + |B|)$ between the amplitudes of the right- and left-traveling wave (white corresponds to right-traveling, black to left-traveling waves). The length of the system is $L = 400$ and the time shown is from $t = 4000$ to $t = 5000$.

Closer to the transition to traveling waves ($h_r = 0.9$) the traveling-wave components become stronger and a characteristic behavior is seen (fig.10). Domains of left-traveling waves expand rapidly to the right for some time until the adjacent right-traveling wave starts to expand rapidly to the left pushing the left-traveling wave back. In the space-time diagram this sequence leads to dark triangles pointing to the right and bright ones to the left. Even for $h_r = 1.1$, i.e. in the regime in which traveling waves of a given wavenumber are stable with respect to standing waves of the same wavenumber, these dynamics of rapid expansion and contraction persist as shown in fig.11.

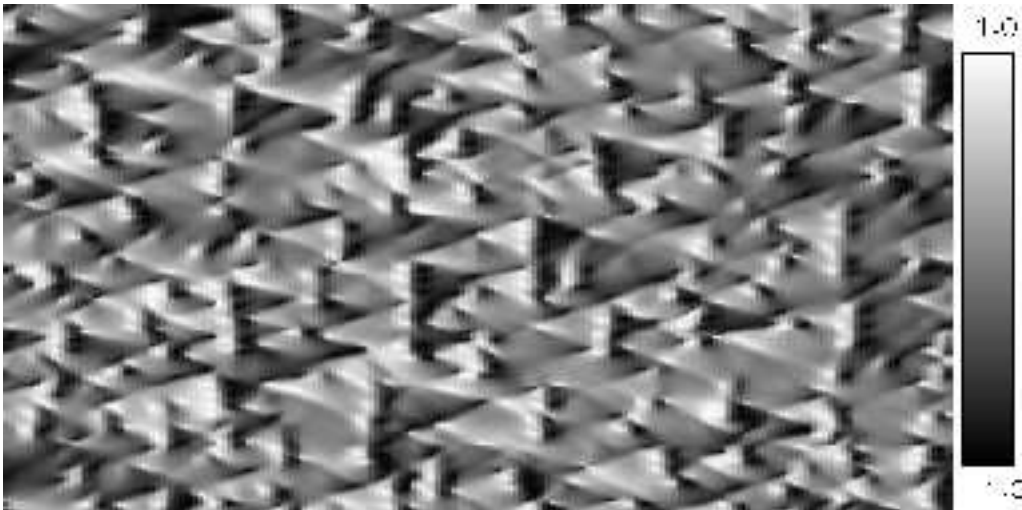


FIG. 10. Space-time diagram (space horizontally, time vertically upward) of evolution obtained by numerical simulation of (1,2) for $h_r = 0.9$. (other parameters as in fig.9).



FIG. 11. Space-time diagram (space horizontally, time vertically upward) of evolution obtained by numerical simulation of (1,2) for $h_r = 1.1$. (other parameters as in fig.9).

The origin of the complex dynamics shown in fig.11 is related to the selection of a non-zero wavenumber by the fronts in $|A|$ and $|B|$, i.e. the sources, combined with the competition of counter-propagating waves of different wavenumbers [29]. A simple calculation shows that right-traveling waves with a wavenumber $p_0 = p_0^{(r)}$ are stable with respect to left-traveling waves with wavenumber $p_0 = 0$ only for

$$(p_0^{(r)})^2 < \mu \frac{h_r - c_r}{h_r}. \quad (49)$$

Beyond this stability limit infinitesimal left-traveling waves are not suppressed by the right-traveling waves and grow. If the instability is only convective the left-traveling waves are swept away and, depending on the size of the domain of right-traveling waves, either perturb the next source or they grow to full amplitude forming a new domain of left-traveling waves. These dynamics ensue if the wavenumber selected by the source [30] is beyond the stability limit given by (49). We have numerically determined the selected wavenumber. As shown in fig.12, it reaches the stability boundary (49) at $h_r = 1.3$. Thus, only for $h_r \geq 1.3$ the wavenumber selected by a source is stable to all counter-propagating waves and the domains of left- and right-traveling waves become stationary and stable. These dynamics have also been discussed recently in the context of an investigation of sources [31].

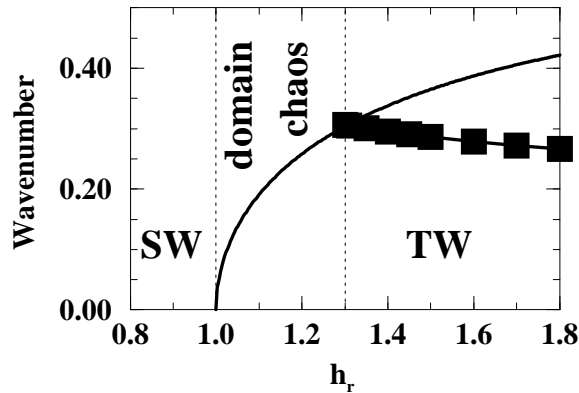


FIG. 12. Wavenumber selected by source (squares) and stability limit of traveling waves with respect to counter-propagating waves (solid line). Between the dotted lines domains of traveling waves are unstable. (Parameters as in fig.9).

V. CONCLUSION

In conclusion, we have performed a detailed stability analysis of standing waves with small group velocity and found behavior that is quite different from that obtained for traveling waves. Due to the group velocity, the analogue of the Eckhaus parabola is shifted with respect to the neutral curve and can be convex from below and convex from above. The unstable solutions can be outside or inside the parabola. In addition, a conservative long-wave instability can arise already at lower order and generically a short-wave instability arises. The Newell-type criterion for the instability of the band-center can be satisfied even for weak dispersion, but it does not indicate the loss of stability of standing waves at all wave numbers.

For group velocities of $O(1)$ the equations discussed here can be viewed as model equations that are obtained by reconstitution of the leading orders in the amplitude expansion. As has been shown previously [23,24,25,26], in the asymptotic limit of small amplitudes non-local equations are obtained. Within the non-local equations the stability properties are considerably simpler. Our detailed analysis of the local (model) equations confirms that the non-local equations are valid immediately above threshold. However, in particular for large systems and for parameters close to the Newell criterion the control-parameter range over which the non-local equations are valid can be extremely small. Thus, already very close to threshold a cross-over can occur to the rich behavior discussed here. A very interesting question is therefore whether this behavior is observable in experimental systems, as might be expected if the cross-over occurs very close to threshold. In nematic liquid crystals the group velocities turn out to be quite small [18,21]. This system is therefore a good candidate to investigate this question.

The stability analysis of standing waves gives sufficient conditions for the instability of traveling rectangles in two dimensions. It is in qualitative agreement with experimental results on spatio-temporally chaotic waves in nematic liquid crystals [14,15,16]. Based on the recent calculation of the nonlinear coefficients in the Ginzburg-Landau equations [21], quantitative comparisons will be possible [22].

In view of the richness of the presented results experiments on rotating convection at small Prandtl numbers are of great interest, since in this system a Hopf bifurcation to standing waves has been predicted [12].

Finally we wish to emphasise that the phenomena treated in this work pertain to spatial modulations (in particular long-wave ones) of the two underlying traveling wave modes. The amplitude degeneracy occurring at $h_r = c_r$ in principle leads to other effects and necessitates the inclusion of higher-order terms [32,33].

Financial support by DFG (Kr690/12) and by DOE (DE-FG02-92ER14303) is gratefully acknowledged.

-
- [1] M. Cross and P. Hohenberg, Rev. Mod. Phys. **65**, 851 (1993).
 - [2] One can rescale the amplitudes in order to have $c_r = 1$, as is often done in the literature. Then one has to replace in all formulas c_i and h by c_i/c_r and h/c_r , respectively.
 - [3] A. Newell, in *Nonlinear Wave Motion*, edited by A. Newell (American Mathematical Society, Providence, RI, 1974), Vol. 15, p. 157.
 - [4] J. Stuart and R. DiPrima, Proc. R. Soc. Lond. A **362**, 27 (1978).
 - [5] B. Matkowsky and V. Volpert, Q. Applied Math. **51**, 265 (1993).
 - [6] M. S. Miguel, Phys. Rev. Lett. **75**, 425 (1995).
 - [7] P. Coullet, S. Fauve, and E. Tirapegui, J. Physique Lett. **46**, 747 (1985).
 - [8] H. Sakaguchi, Prog. Theor. Phys. **93**, 491 (1995).
 - [9] E. Knobloch, in *Nonlinear dynamics and pattern formation in the natural environment*, edited by A. Doelman and A. van Harten (Longman, 1995).
 - [10] H. Riecke, Europhys. Lett. **11**, 213 (1990).
 - [11] I. Rehberg and G. Ahlers, in "Contemporary Mathematics", Vol. 56 (1986).
 - [12] T. Clune and E. Knobloch, Phys. Rev. E **47**, 2536 (1993).
 - [13] L. Kramer and W. Pesch, in *Pattern formation in liquid crystals*, edited by A. Buka and L. Kramer (Springer, New York, 1996), Chap. Electrohydrodynamic instabilities in nematic liquid crystals.
 - [14] M. Dennin, D. Cannell, and G. Ahlers, Mol. Cryst. Liq. Cryst. **261**, 337 (1995).
 - [15] M. Dennin, G. Ahlers, and D. Cannell, Science **272**, 388 (1996).
 - [16] M. Dennin, D. Cannell, and G. Ahlers, Phys. Rev. E **57**, 638 (1998).
 - [17] M. Silber, H. Riecke, and L. Kramer, Physica D **61**, 260 (1992).
 - [18] M. Treiber and L. Kramer, Mol. Cryst. Liq. Cryst. **261**, 311 (1995).
 - [19] M. Dennin *et al.*, Phys. Rev. Lett. **76**, 319 (1996).

- [20] M. Treiber, N. Eber, A. Buka, and L. Kramer, J. Phys. II **7**, 649 (1997).
- [21] M. Treiber and L. Kramer, Phys. Rev. E **58**, 1973 (1998).
- [22] M. Treiber, H. Riecke, and L. Kramer, unpublished .
- [23] E. Knobloch and J. D. Luca, Nonlinearity **3**, 975 (1990).
- [24] E. Knobloch, in *Pattern Formation in Complex Dissipative Systems*, edited by S. Kai (World Scientific, Singapore, 1992).
- [25] B. Matkowsky and V. Volpert, Physica D **54**, 203 (1992).
- [26] J. Vega, SIAM J. Math. Anal. **24**, 603 (1993).
- [27] C. Martel and J. Vega, Nonlinearity **9**, 1129 (1996).
- [28] C. Martel and J. Vega, Nonlinearity **11**, 105 (1998).
- [29] H. Riecke and I. Aranson, unpublished .
- [30] B. Malomed, Phys. Rev. E **50**, 3310 (1994).
- [31] M. van Hecke, C. Strom, and W. van Saarloos, Physica D (submitted).
- [32] J. Crawford and E. Knobloch, Physica D **31**, 1 (1988).
- [33] M. Golubitsky and M. Roberts, J. Differ. Equ. **69**, 216 (1987).